Human medullary responses to cooling and rewarming the skin: A functional MRI study

Robin M. McAllen*†‡, Michael Farrell*§, John M. Johnson¶, David Trevaks*, Leonie Cole*, Michael J. McKinley*, Graeme Jackson‖, Derek A. Denton††‡‡, and Gary F. Egan*§**

*Howard Florey Institute of Experimental Physiology and Medicine, §Centre for Neuroscience, and Departments of ††Physiology and †Anatomy and Cell Biology, University of Melbourne, Melbourne, Victoria 3010, Australia; ¶Department of Physiology, University of Texas Health Sciences Center, San Antonio, TX 78229; ‖Brain Research Institute, Austin Health, West Heidelberg, Victoria 3084, Australia; and **Baker Heart Research Institute, Alfred Hospital, Prahran, Victoria 3181, Australia

Contributed by Derek A. Denton, November 12, 2005

A fall in skin temperature precipitates a repertoire of thermoregulatory responses that reduce the likelihood of a decrease in core temperature. Studies in animals suggest that medullary raphé neurons are essential for cold-defense, mediating both the cutaneous vasoconstrictor and thermogenic responses to ambient cooling; however, the involvement of raphé neurons in human thermoregulation has not been investigated. This study used functional MRI with an anatomically guided region of interest (ROI) approach to characterize changes in the blood oxygen level-dependent (BOLD) signal within the human medulla of nine normal subjects during non-noxious cooling and rewarming of the skin by a water-perfused body suit. An ROI covering 4.9 ± 0.3 mm² in the ventral midline of the medulla immediately caudal to the pons (the rostral medullary raphé) showed an increase in BOLD signal of 3.9% ($P < 0.01$) during periods of skin cooling, compared with other times. Overall, that signal showed a strong inverse correlation ($R = 0.48$, $P < 0.001$) with skin temperature. A larger ROI covering the internal medullary cross section at the same level (area, 126 ± 15 mm²) showed no significant change in mean BOLD signal with cooling (+0.2%, $P > 0.05$). These findings demonstrate that human rostral medullary raphé neurons are selectively activated in response to a thermoregulatory challenge and point to the location of thermoregulatory neurons homologous to those of the raphé pallidus nucleus in rodents.

functional neuroimaging | raphé | rostral medulla | thermoregulation

In birds and mammals, effective mechanisms have evolved to regulate heat loss and heat production and to maintain body temperature within a limited range. A series of hierarchically organized reflexes act to normalize body temperature: these are driven by thermal detectors of superficial (skin) and deep body temperature (1). Invasive experiments in mammals have established that the dominant detectors of deep body temperature are located in the brain, primarily in the anterior hypothalamus/preoptic area, although receptors in the spinal cord and elsewhere also contribute (2). Although the same is presumed to apply to humans, direct evidence is lacking. Recent studies on rats (3–7) and rabbits (8, 9) have now also found that a small brainstem nucleus, the medullary raphé, is a key synaptic relay in the efferent pathways of several heat-conserving mechanisms that are engaged by exposure to cold. Whether these findings on furred animals apply also to humans is unknown.

Humans have proved to be an ideal species in which to investigate thermoregulatory mechanisms by noninvasive methods. Such studies have established that, during exposure to a moderately cold environment, skin receptors provide effective feed-forward control of body temperature, such that deep body temperature not only is prevented from falling but often rises (10). Detailed studies have also demonstrated functional interaction between deep body and skin temperatures in the control of thermoregulatory effector mechanisms (11, 12).

Several functional imaging studies have followed the human brain response to noxious and non-noxious cooling or heating of small skin areas (e.g., the hand). These have revealed brain pathways involved in pain and temperature perception (13). To engage thermoregulatory mechanisms, however, larger skin areas generally need to be stimulated or deep body temperature needs to be altered. In one such study, ^{18}F-flurodeoxyglucose positron emission tomography was used to investigate brain metabolism during steady state hyperthermia (14). Compared with the resting normothermic state, hyperthermia was associated with an overall increase in cerebral metabolism, with specific increases noted in the hypothalamus, thalamus, corpus callosum, cingulate gyrus, and cerebellum (14). In a second study, functional MRI provided evidence on the brain regions involved in body temperature sensation. In this case the amygdala showed significant activation correlated with the sensation of thermal discomfort during exposure of the whole body to cold air (15).

No study has specifically investigated the involvement in human thermoregulation of the brainstem, and studies of the brainstem using functional MRI are in their infancy. The application of functional MRI to investigate brainstem responses has been hampered by a number of technical challenges, including magnetic susceptibility and movement-related artifacts. In addition, no suitable neuroimaging brainstem atlas exists. The limitation of applying existing registration algorithms to brainstem structures has prompted us and others (16–18) to take new approaches. In this regard, a recent study has developed approaches that successfully imaged structures at the pontomedullary junction activated by cutaneous and visceral pain (19).

The present investigation was prompted by the demonstration in animal studies that medullary raphé neurons are critically involved in thermoregulatory responses to cold (see above). The neurons responsible occupy a ventral midline region, level with the caudal parts of the facial nuclei. We wished to investigate the responses of the human homologue of this spatially discrete region to non-noxious cooling of the body surface. We investigated the raphé response by an anatomically focused region of interest (ROI) analysis method. We hypothesized that cooling the skin with a body suit would activate the medullary raphé and that the activation would be localized rather than part of a more general medullary response.

Results

Skin Temperature and Ratings of Skin Temperature. Cold water was circulated through the tube suit for two 5-min periods, during

Conflict of interest statement: No conflicts declared.

Abbreviations: BOLD, blood oxygen level-dependent; ROI, region of interest.

‡To whom correspondence may be sent at the * address. E-mail: rmca@hfi.unimelb.edu.au.

‡‡To whom correspondence may be sent at the †† address. E-mail: d.denton@hfi.unimelb.edu.au.

which skin temperature fell from 33.1 ± 0.1 to 28.7 ± 0.6°C and from 31.2 ± 0.2 to 27.5 ± 0.6°C (Fig. 1*G*). Subjective appraisals of skin temperature (Fig. 1*H*) correlated with measured skin temperature (average correlation coefficient $r = 0.47$; range, 0.06–0.68). Although most subjects perceived the maximum stimulus as "very cold," none considered it painful.

Raphé and Medullary Cross Section ROIs. The anatomically targeted raphé ROI occupied 4.9 ± 1.1 mm^2 of the most rostral axial slice of the medulla, corresponding to a volume of 10.0 ± 3.3 mm^3. The second ROI, incorporating the internal cross section of the same medullary slice, had a surface area of 127 ± 46 mm^2, corresponding to a volume of 265 ± 138 mm^3 (mean ± SD in each case). Fig. 1 *A–D* shows the ROI locations. Any movement within the plane of the slice was compensated manually by adjusting the position of the template, as described in *Methods*. No compensation was made for between-slice movements, but in every case the maximum displacement was less than the thickness of the slice.

The mean BOLD signal intensity of the raphé ROI during the two cooling periods was significantly greater than the mean intensity during noncooling periods (3.9% mean signal change between baseline and rewarming periods, $P < 0.01$). By contrast, the signal from the medullary cross section ROI was not significantly different between cooling and noncooling periods (0.2% signal change, $P > 0.05$) (Fig. 1*E*).

The time course of the raphé BOLD signal is shown in relation to skin temperature and temperature perception ratings in Fig. 1 *F–H*. Compared with the first cooling period, the greater fall in skin temperature during the second cooling period (Fig. 1*G*) was matched by a higher BOLD signal (Fig. 1*F*). A striking decline in the raphé BOLD signal is evident at the start of each rewarming period. Subjective skin temperature ratings also reversed rapidly upon rewarming (Fig. 1*H*). Overall, the group mean raphé BOLD signal was inversely correlated with skin temperature ($R = 0.48$, $P < 0.001$).

Discussion

Thermal receptors on the human skin are important not only for thermal sensation but also for thermoregulation. Cutaneous cold receptors thus provide feed-forward signals for the coordinated heat-conservation and heat-generation responses that are engaged by the body in a cold environment. It is therefore predictable that thermal stimulation of the skin should activate not only brain regions implicated in thermal sensation [e.g., thalamus and insular cortex (20)] but also those concerned with thermoregulation. Most previous human imaging studies have applied brief thermal stimuli to small skin areas and focused on thermal sensory responses (21, 22). We chose to cool a large skin area over several minutes, a form of stimulus that is likely to emphasize thermoregulatory responses. We found that this caused a robust increase in the BOLD signal of the medullary raphé, an increase that was anatomically localized rather than part of a more generalized brainstem activation. The hypothesis that raphé neurons show a specific, graded response to body cooling was further supported by the strong inverse correlation between the raphé BOLD signal and skin temperature.

The raphé BOLD signal and the subjective ratings of thermal sensation both demonstrated a steep reversal at the start of rewarming, a pattern consistent with the inhibitory effects of skin warming on the discharge of cutaneous cold receptors (23, 24). Only cutaneous cold receptors would have been involved, because the degree of cooling was confined to the non-noxious range (25–27). The primary stimulus in this experiment was undoubtedly skin temperature. Although core temperature was not measured in the magnet, mild surface cooling generally causes a small overcompensation in core body temperature (10). A single comparable cooling episode in a previous study using the same cooling method (28) also caused a nonsignificant rise in oral temperature at the time of minimum skin temperature. Oral temperature subsequently fell slightly during the recovery (rewarming) period of that study, however (28), so we cannot exclude the possibility that a similar fall in core temperature carried over into the second cooling episode of the present study, contributing to its stronger raphé BOLD response. If so, this would have acted in synergy with the primary stimulus, cool skin (29).

There are pitfalls associated with imaging small regions close to brain–cerebrospinal fluid interfaces, where the high BOLD signal of the cerebrospinal fluid may be mixed with the lower signal from the brain parenchyma. This mixing can happen as a consequence of voxel resampling and interpolation during preprocessing steps, such as motion correction and spatial normalization. To prevent such artifacts we avoided all automated preprocessing steps and used the raw echoplanar images in native space. Our manual approach allowed us to compensate for any movement in the plane of the cross-sectional slice of brainstem and to ensure that the raphé and medullary ROIs stayed clear of the nearby ventral brain margin throughout the measurement series. As noted above, any between-slice movement was within the thickness of the slice. This approach ensured that the signals that were detected in the present study were not caused by movement-related artifacts associated with the brainstem surface.

By means of an anatomically targeted ROI analysis, we were able to identify a robust increase in the BOLD signal from a highly localized region in the medulla when the skin was cooled. This signal was distinct from any more generalized signal change in proximate tissues, as demonstrated by the lack of a significant difference in the signal from the medullary cross section between the cooling and noncooling periods. The magnitude of the raphé BOLD response was greater than those generally reported for human cortical BOLD responses, although comparable with brainstem BOLD responses reported by others (18, 19) and less than was reported to occur in optimally designed animal studies (30). It appears that the anatomically guided choice of ROI has accurately identified the most responsive region, delivering a signal that is undiluted by contributions from neighboring unresponsive, or inversely responsive, areas. Additionally, or alternatively, the small ROI could have incorporated a significant contribution from veins draining the midline raphé region. If so, the neurons responsible for the BOLD signal increase may have been situated slightly more dorsal to our ROI, given that the blood supply to this region flows from and to the ventral brainstem surface (31).

The rationale for the focus on the raphé is firmly based on data from animal studies. Neurons in this region are strongly activated by cutaneous or ambient cooling, as demonstrated by expression of the immediate early gene product Fos after cold-exposure in conscious rats (3, 32) and by electrophysiological recordings in anesthetized rats (33, 34). Evidence from rats has also demonstrated a critical role for raphé neurons in the cutaneous vasoconstrictor and nonshivering thermogenic responses (by means of sympathetic drive to brown adipose tissue) to cold. Microinjections of inhibitory neurotransmitter agonists (which act on cell bodies but not fiber tracts) into the raphé can prevent cold-induced sympathetic drives to cutaneous blood vessels (7) and to brown adipose tissue (3) and cause a failure to maintain body temperature in a cool environment (35). The critical region for these effects is depicted on the cross section of the rostral rat medulla shown in Fig. 1*I*. Although the physiological response to non-noxious cooling involves redistribution of blood flow from the body shell to the core, with reciprocal vasomotor adjustments to cutaneous and noncutaneous vessels (36), it is unlikely that the vasomotor control pathways to noncutaneous vessels involve the medullary raphé (37, 38). With regard to thermosensory processes, no clear evidence implicates the direct involvement of medullary raphé neurons, although raphé involvement in as-

cending thermosensory processing has been suggested (2, 33). In fact, the known ascending tracts that convey cold information to the thalamus and forebrain (lamina I spinothalamic projections) follow a lateral path through the brainstem (39). These considerations, in combination with other data that implicate raphé involvement also in descending pathways from the preoptic area (5, 40, 41), make it most likely that raphé neurons act as a synaptic relay in efferent pathways for cold defense.

The ROI in the ventral medullary raphé was chosen to match, as closely as possible, the region in the rat medulla where temperature-sensitive neurons and thermoregulatory pathways have been localized. In the rat, the critical site is considered by some workers to be the raphé pallidus nucleus (3), although others consider that neighboring neurons may also contribute to the function (8, 9). The raphé pallidus nucleus in rats and rabbits coincides with a dense concentration of serotonergic neurons, whose role in thermoregulatory responses is a matter of active debate (42). Serotonergic neurons have also been implicated in several other homeostatic functions, including the chemical drive to breathe (43). An alternative view is that glutamatergic cells expressing the vesicular glutamate transporter VGLUT-3 are the cells responsible (although a minority of these may also express a serotonergic phenotype) (6). In humans, Kinney and colleagues (44, 45) consider that the neurons homologous with the rodent raphé pallidus nucleus occupy an anatomically similar region, dorsomedial to the pyramids, as well as a further ventral extension into the arcuate nucleus (which does not exist in rats). The main concentration of medullary serotonergic neurons in humans, however, is located elsewhere, dorsal to the medial lemnisci (46). Our observations suggest that the thermoregulatory neurons in humans coincide with the anatomic homolog (the nucleus raphé pallidus/dorsal part of arcuate nucleus) rather than the main serotonergic cell group. It would be interesting to know whether human raphé pallidus/arcuate neurons express the VGLUT-3 phenotype identified in the homologous rodent neurons involved in cold-defense (6), but this has not yet been investigated. As noted, however, we cannot exclude the possibility that venous drainage from neurons located more dorsally, perhaps including the main serotonergic group, contributed to the BOLD signal of our raphé ROI.

The significance of these findings is that we have localized in the human brainstem a nucleus that responds to whole-body cooling and is thus central to the control of a bodily function crucial to human survival: thermoregulation. The thermoregulatory response of the raphé in humans is most likely to be a rate-dependent cold-defense mechanism whereby the raphé output increases unidirectionally with decreasing skin temperature. We have also revealed an interesting anatomical homology between rats and humans, finding the human raphé thermoregulatory region in the ventral part of the rostral medullary midline, dorsomedial to the pyramids. By measuring thermal intensity we have also seen a relationship between the raphé response and higher cortical processes that are involved in perception. However, further studies are needed to fully elucidate the complex relationship among brainstem thermoregulatory mechanisms, skin temperature perception, and thermal comfort.

Methods

The sample for the study consisted of 10 subjects (6 males and 4 females) with a mean age of 35.9 ± 10.8 years (range 22–55). All subjects gave informed consent consistent with processes approved by the Human Research Ethics Committee of the Howard Florey Institute.

Temperature Control and Measurement. Temperature-controlled water was pumped through a garment incorporating a network of small-diameter plastic tubing. The garment covered the arms to the wrists, the legs to the ankles, and the torso. Skin temperature at its interface with the garment was recorded at 30-s intervals as an integrated signal from three thermocouples taped to the abdomen below the umbilicus, the central lumbar area, and the anterior thigh. Subjects rated skin temperature on a −4 to +4 scale at a frequency of once per minute. The ratings were denoted very cold, cold, cool, slightly cool, neutral, slightly warm, warm, hot, and very hot, respectively. Verbal prompts for ratings were made through the scanner intercom system. Subjects indicated their ratings by extending the corresponding number of fingers (left hand cool, right hand warm). The experimental paradigm consisted of five 5-min periods in the following order: baseline at or close to thermoneutrality (neutral water reservoir at 31–33°C), cooling (cold water reservoir at 2–4°C), rewarming (neutral reservoir), cooling (cold reservoir), and rewarming (neutral reservoir). Water was pumped from the reservoir around a circuit through 9-m lengths of plastic tubing to and from the tube suit. The water took 30 s to travel from the reservoir to the tube suit.

Image Acquisition. Anatomical and functional images were collected with a 3-tesla Magnetic Resonance scanner (General Electric) at the Brain Research Institute (Melbourne). Anatomical images were acquired in a sagittal orientation (time to repetition, 14 ms; time to echo, 2.8 ms; 512 × 256 matrix; field of view, 240 mm; slice thickness, 2 mm; voxel size after interpolation of matrix data, 2.00 × 0.47 × 0 .47 mm^3). Echoplanar images were also acquired in the sagittal plane (time to repetition, 5 s; time to echo, 40 ms; flip angle (FA), 60°; 128 × 128 matrix; field of view, 240 mm; slice thickness, 3 mm with 0.5-mm interslice gap; voxel size, 3.00 × 1.88 × 1.88 mm^3) on 300 occasions during the course of 25 min of scanning. Two subjects were scanned with a high-resolution functional imaging sequence. The high-resolution sequence consisted of a time series of 150 echoplanar images acquired in the axial plane from a partial brain volume incorporating the brainstem (time to repetition, 10 s; time to echo, 33.9 ms; FA, 90°; 128 × 128 matrix; field of view, 140 mm; slice thickness, 2 mm with 0.5-mm interslice gap; voxel size, 2.00 × 1.09 × 1.09 mm^3).

Image Analysis. The circumscribed spatial extent of the ROIs and their locality did not permit accurate coregistration across subjects, given the constraints of current movement correction and normalization algorithms. We did, however, use SPM (Wellcome Department of Cognitive Neurology, London) to quantify movements of each subject during scanning, but no movement correction was made to the data. ROIs were defined according to anatomical features on the echo planar image (EPI) on a case-by-case basis. In every case, we chose the most rostral axial slice of the medulla before the appearance of the pons. Each volume of the chosen slice was then exported [by using MRICRO (48)] into individual graphic files (TIFF), and then every pixel was subdivided (using PHOTOSHOP, Adobe Systems, San Jose, CA) by 16 (4 × 4) to improve the localization of template placement. By using the first scan in the series, templates were drawn of the perimeter of the brainstem, the internal cross section of the medulla, and the raphé, based on the individual subject's anatomy. The region chosen to represent the medullary raphé was centered on the midline, immediately dorsomedial to the pyramids (Fig. 1*D* and *I*). The region chosen to represent the signal from the internal medullary cross section was drawn immediately inside the brainstem perimeter, avoiding surface voxels (Fig. 1*C*). The templates, for both the cross section of the medulla and raphé, were then carefully placed in the appropriate position on each sequential scan, allowing for any movement. Once the template was in position, the mean luminosity was recorded for the raphé ROI and medullary cross section ROI. Sequential

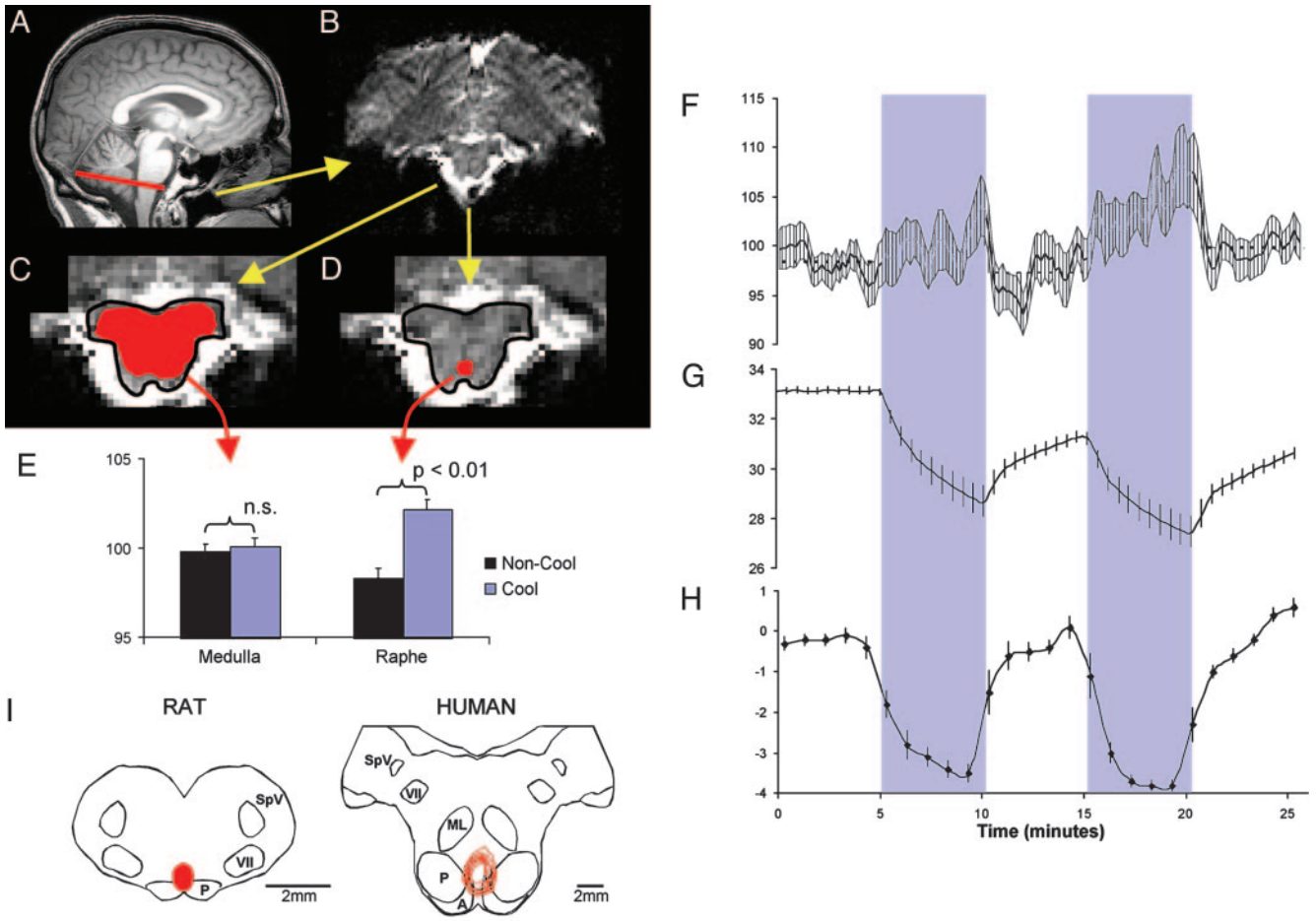

Fig. 1. Figure showing process for definition of ROIs, responses to skin cooling, and comparative functional anatomy of medullary raphé. (*A*) Midline sagittal T1-weighted brain image, indicating the rostral medullary slice containing the ROIs (red line). (*B*) Echoplanar MRI of the rostral medullary slice in the same subject showing the dorsal surface at the top of the image. (*C* and *D*) Expanded view of the brainstem from *B*, highlighting the medullary outline (drawn in black) and the medullary (*C*) and raphé (*D*) ROIs drawn in red. (*E*) Histogram of mean BOLD signal from the medullary and raphé ROIs during cooling (blue bars) and noncooling (black bars) periods in nine subjects. Significant differences are indicated. (*F–H*) Time profiles of the mean raphé BOLD signal (*F*), mean skin temperature (*G*), and mean subjective ratings of skin thermal sensation (*H*) in nine subjects. The two 5-min cooling periods in the protocol are indicated by a blue stippled background. In all panels, the error bars denote SEM. (*I Left*) Cross section drawing of rat rostral medulla, indicating the region found to be essential for cold-driven vasoconstriction and thermogenesis [the red area indicates the overlying raphé pallidus nucleus (3, 7)]. (*I Right*) Corresponding section of human medulla (drawn with reference to Blessing (ref. 47, p. 379) and Duvernoy (ref. 31, pp. 54 and 123) on which are plotted (in red) the nine raphé ROIs analyzed in the present study. A, arcuate nucleus; ML, medial lemnicus; P, pyramidal tract; SpV, spinal trigeminal nucleus; VII, facial nucleus.

luminosity values from each ROI in each subject were expressed as a percentage of its value in the first image of the series. The pixel areas of the medullary cross section and raphé ROIs were recorded for each individual subject. The images of the medulla from one male subject were too distorted to permit accurate definition of the ROI. These data were therefore discarded, and further analysis was performed on the mean data from five male and four female subjects.

The mean blood oxygen level-dependent (BOLD; luminosity) signal from each ROI during cooling periods was compared with the mean signal from all other times by paired *t* test. Linear regression was used to test the relation between the mean raphé BOLD signal and the mean skin temperature every 10 s throughout the 25-min protocol (skin temperature was interpolated to fill gaps between actual readings). $P < 0.05$ was considered significant.

We are grateful to Bill Blessing for illuminating discussions on brainstem functional anatomy. This work was supported by the National Health and Medical Research Council of Australia, the Search Foundation, the Brown Foundation, the Harold G. and Leila Y. Mathers Charitable Foundation, and the Robert J. Jr. and Helen C. Kleberg Foundation.

1. Satinoff, E. (1978) *Science* **201,** 16–22.
2. Simon, E., Pierau, F. K. & Taylor, D. C. (1986) *Physiol. Rev.* **66,** 235–300.
3. Morrison, S. F. (2004) *News Physiol. Sci.* **19,** 67–74.
4. Morrison, S. F., Ramamurthy, S. & Young, J. B. (2000) *J. Neurosci.* **20,** 9264–9271.
5. Tanaka, M., Nagashima, K., McAllen, R. M. & Kanosue, K. (2002) *J. Physiol.* **540,** 657–664.
6. Nakamura, K., Matsumura, K., Hubschle, T., Nakamura, Y., Hioki, H., Fujiyama, F., Boldogkoi, Z., Konig, M., Thiel, H. J., Gerstberger, R., *et al.* (2004) *J. Neurosci.* **24,** 5370–5380.
7. Ootsuka, Y., Blessing, W. W. & McAllen, R. M. (2004) *Neurosci. Lett.* **357,** 58–62.
8. Ootsuka, Y. & Blessing, W. W. (2005) *Brain Res.* **1051,** 189–193.
9. Blessing, W. W., Yu, Y. H. & Nalivaiko, E. (1999) *Neurosci. Lett.* **270,** 33–36.
10. Savage, M. V. & Brengelmann, G. L. (1996) *J. Appl. Physiol.* **80,** 1249–1257.
11. Johnson, J. M., O'Leary, D. S., Taylor, W. F. & Park, M. K. (1984) *J. Appl. Physiol.* **56,** 1283–1288.
12. Pergola, P. E., Johnson, J. M., Kellogg, D. L., Jr., & Kosiba, W. A. (1996) *Am. J. Physiol.* **270,** H208–H215.
13. Farrell, M. J., Laird, A. R. & Egan, G. F. (2005) *Hum. Brain Mapp.* **25,** 129–139.

14. Nunneley, S. A., Martin, C. C., Slauson, J. W., Hearon, C. M., Nickerson, L. D. & Mason, P. A. (2002) *J. Appl. Physiol.* **92,** 846–851.
15. Kanosue, K., Sadato, N., Okada, T., Yoda, T., Nakai, S., Yoshida, K., Hosono, T., Nagashima, K., Yagishita, T., Inoue, O., *et al*. (2002) *Neurosci. Lett.* **329,** 157–160.
16. Borsook, D., DaSilva, A. F., Ploghaus, A. & Becerra, L. (2003) *J. Neurosci.* **23,** 7897–7903.
17. DaSilva, A. F., Becerra, L., Makris, N., Strassman, A. M., Gonzalez, R. G., Geatrakis, N. & Borsook, D. (2002) *J. Neurosci.* **22,** 8183–8192.
18. Topolovec, J. C., Gati, J. S., Menon, R. S., Shoemaker, J. K. & Cechetto, D. F. (2004) *J. Comp. Neurol.* **471,** 446–461.
19. Dunckley, P., Wise, R. G., Fairhurst, M., Hobden, P., Aziz, Q., Chang, L. & Tracey, I. (2005) *J. Neurosci.* **25,** 7333–7341.
20. Craig, A. D. (2002) *Nat. Rev. Neurosci.* **3,** 655–666.
21. Craig, A. D., Chen, K., Bandy, D. & Reiman, E. M. (2000) *Nat. Neurosci.* **3,** 184–190.
22. Davis, K. D., Kwan, C. L., Crawley, A. P. & Mikulis, D. J. (1998) *J. Neurophysiol.* **80,** 1533–1546.
23. Campero, M., Serra, J., Bostock, H. & Ochoa, J. L. (2001) *J. Physiol.* **535,** 855–865.
24. Darian-Smith, I., Johnson, K. O. & Dykes, R. (1973) *J. Neurophysiol.* **36,** 325–346.
25. Verdugo, R. & Ochoa, J. L. (1992) *Brain* **115,** 893–913.
26. Harrison, J. L. & Davis, K. D. (1999) *Pain* **83,** 123–135.
27. Campero, M., Serra, J. & Ochoa, J. L. (1996) *J. Physiol.* **497,** 565–572.
28. Egan, G. F., Johnson, J., Farrell, M., McAllen, R., Zamarripa, F., McKinley, M. J., Lancaster, J., Denton, D. & Fox, P. T. (2005) *Proc. Natl. Acad. Sci. USA* **102,** 5262–5267.
29. Owens, N. C., Ootsuka, Y., Kanosue, K. & McAllen, R. M. (2002) *J. Physiol.* **543,** 849–858.
30. Mandeville, J. B., Marota, J. J., Ayata, C., Moskowitz, M. A., Weisskoff, R. M. & Rosen, B. R. (1999) *Magn. Reson. Med.* **42,** 944–951.
31. Duvernoy, H. (1978) *Human Brainstem Vessels* (Springer, Berlin).
32. Bonaz, B. & Tache, Y. (1994) *Brain Res.* **652,** 56–64.
33. Dickenson, A. H. (1977) *J. Physiol.* **273,** 277–293.
34. Rathner, J. A., Owens, N. C. & McAllen, R. M. (2001) *J. Physiol.* **535,** 841–854.
35. Zaretsky, D. V., Zaretskaia, M. V. & DiMicco, J. A. (2003) *Am. J. Physiol.* **285,** R110–R116.
36. Kregel, K. C., Seals, D. R. & Callister, R. (1992) *J. Physiol.* **454,** 359–371.
37. Morrison, S. F. (1999) *Am. J. Physiol.* **276,** R962–R973.
38. Rathner, J. A. & McAllen, R. M. (1999) *Brain Res.* **834,** 196–199.
39. Craig, A. D. (1995) *J. Comp. Neurol.* **361,** 225–248.
40. Morrison, S. F. (2003) *Neuroscience* **121,** 17–24.
41. Nakamura, K., Matsumura, K., Kaneko, T., Kobayashi, S., Katoh, H. & Negishi, M. (2002) *J. Neurosci.* **22,** 4600–4610.
42. Ootsuka, Y. & Blessing, W. W. (2005) *Am. J. Physiol.* **288,** R909–R918.
43. Richerson, G. B. (2004) *Nat. Rev. Neurosci.* **5,** 449–461.
44. Kinney, H. C., Filiano, J. J. & White, W. F. (2001) *J. Neuropathol. Exp. Neurol.* **60,** 228–247.
45. Zec, N., Filiano, J. J. & Kinney, H. C. (1997) *J. Neuropathol. Exp. Neurol.* **56,** 509–522.
46. Halliday, G. M., Li, Y. W., Joh, T. H., Cotton, R. G., Howe, P. R., Geffen, L. B. & Blessing, W. W. (1988) *J. Comp. Neurol.* **273,** 301–317.
47. Blessing, W. W. (1997) *The Lower Brainstem and Bodily Homeostasis* (Oxford Univ. Press, New York).
48. Rorden, C. & Brett, M. (2000) *Behav. Neurol.* **12,** 191–200.